The role of conductivity and molecular mobility on the photoanisotropic response of a new azo-polymer containing sulfonic groups.

Sakinah Mohd Alauddin[1,2], Nurul Fadhilah Kamalul Aripin[1,2], T.S. Velayutham[2,3], Irakli Chaganava[4, 5], Alfonso Martinez-Felipe[6, *]

[1] Faculty of Chemical Engineering, University of Technology MARA, 40450 Shah Alam, Selangor Darul Ehsan, Malaysia.

[2]Fundamental and Frontier Sciences in Nanostructure Self-Assembly Center, Department of Chemistry, Faculty of Science, University of Malaya, 50603 Kuala Lumpur, Malaysia.

[3] Low Dimensional Material Research Center, Department of Physics, Faculty of Science, University of Malaya, 50603 Kuala Lumpur, Malaysia.

[4] Laboratory of Holographic Recording and Processing of Information, Institute of Cybernetics, GTU. 5 Sandro Euli str., 0186 Tbilisi. Georgia.

[5] Georgian State Teaching University of Physical Education and Sport.49, Chavchavadze ave. 0179, Tbilisi. Georgia.

[6] Chemical and Materials Engineering Research Group, School of Engineering, University of Aberdeen, King's College, Old Aberdeen AB24 3UE, UK.

* Corresponding author: a.martinez-felipe@abdn.ac.uk

Keywords: azo-polymers; dielectric spectroscopy; UV-Vis spectrophotometry; photoanisotropy; *trans*-to-*cis* photoisomerisation; conductivity.

Abstract

We report the preparation of a new light-responsive side-chain terpolymer containing azobenzenes, as chromophoric components, sulfonic groups, as polar components, and methacrylate groups, as film forming components, and we provide a detailed characterisation of its thermal parameters, photoanisotropic character, dielectric response and optoelectronic properties. The poly[(4-methoxyazobenzene -4'-oxy) methacrylate]-*co*-poly[2-acrylamido-2-methyl-1-propanesulfonic acid]-*co*-poly[methyl methacrylate], MeOAzB/AMPS/MMA, was prepared by radical copolymerisation, possesses high thermal stability and is amorphous. Its high glass transition (T_g = 151^{o}C) is explained by steric effects (induced by the bulky azobenzenes) and hydrogen bonding (promoted by the polar sulfonic groups) near the polymeric backbone, which may also reduce the photoanisotropic efficiency. The transition between the energy levels of the azobenzenes (MeOAzB) in the terpolymer is controlled by p-type conductivity, and can be associated to motions in the side-chains containing the sulfonic groups (AMPS), which are locally activated below the MeOAzB/AMPS/MMA glass transition.

1. Introduction

Azobenzenes are undoubtedly some of the most utilised and investigated components as light-responsive materials, based on their *trans*-to-*cis* photoisomerisation driven by irradiation with UV light, normally around ~ 365 nm, see **Fig. 1** [1, 2]. This process is reversible, and the *cis*-to-*trans* relaxation to the ground state can occur by thermal activation, and can also be promoted by irradiation at longer wavelengths. Due to the molecular anisotropy of the *trans* isomers, azobenzenes can assist the formation of liquid crystalline phases, and are used to disrupt the order in microstructures by switching to the non-linear *cis* isomer [3]. The application of light allows for spatial control with high efficiency, and a wide variety of so-called azo-polymers have been extensively prepared and used for data storage [4-11], in plasmonic metasurfaces for photopatterning of molecular orientations[12], as electrolytes with enhanced ionic transport [13-18], in formulations for controlled drug delivery [19-23] and as energy harvesters [24, 25].

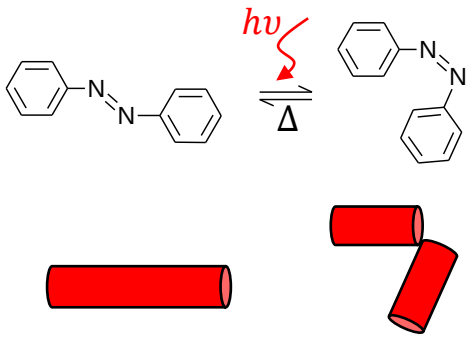

Figure 1. Azobenzene isomers: *trans* (left) and *cis* (right). *Trans*-to-*cis* isomerisation, triggered by UV-Vis light radiation (h*v*), and thermally activated *cis*-to-*trans* relaxation (Δ).

Photoanisotropy is an attractive strategy to exert directional control on the morphological changes of azo-compounds that respond to actinic linearly polarised light. In addition, operation in a narrow band of the electromagnetic spectrum allows to encode a photo signal with very high density[26]. Photoanisotropic materials are particularly relevant in the production of polarisation-holographic elements [27], which can carry out analyses and transformations of light in real time and to operate in a wide spectral range. As a result, a single polarisation-holographic element can replace an entire set of conventional elements in polarisation optics.

Organic media based on polymers and functional azo-dyes are increasingly popular as holographic elements, and recently, we have developed side-chain copolymers containing

azobenzenes that show promising, but unusual, photochromic response in terms of photoanisotropy ($A_{eff\ Max}$) and induction velocity ($\dot{A_{eff}}$, s^{-1}) [28]. The polarity of these materials relies on the presence of terminal cyano groups attached to the azobenzene units, which increase their photosensitivity and accelerate the response to actinic light through intramolecular push-pull effects. Unfortunately, uncontrolled self-aggregation resulted in inhomogeneous samples with low values of optical isotropy. In order to yield homogeneous films with thickness around 20 μm, it was then necessary to mix the azo-materials with a non-chromophore polymer, resulting in poorer photoanisotropic parameters.

In the present work, we investigate new photoanisotropic polymers that contain azobenzene and polar groups in different side-chains of a poly(methacrylate)-based terpolymer: the poly[(4-methoxyazobenzene -4'-oxy) methacrylate]-*co*-poly[2-acrylamido-2-methyl-1-propanesulfonic acid]-*co*-poly[methyl methacrylate], MeOAzB/AMPS/MMA, ***1*** in **Fig. 2**. The methoxyazobenzene units, MeOAzB, promote optoelectronic response, whilst the 2-acrylamido-2-methyl-1-propanesulfonic acids, AMPS, contain polar sulfonic groups. Methyl(methacrylate) groups, MMA, are introduced into the main chain in order to enhance the film forming properties. Our target is to enhance the optoelectronic performance of new polymeric azo-derivatives by the inclusion of the AMPS groups, based on the high conductivity observed in analogous materials [29, 30]. With this strategy, we aim to facilitate mutual integration of polar components that can accelerate the light response of azobenzenes by forming specific interactions, while maintaining design flexibility. Here we have evaluated such effects by a full structural, dielectric and conductivity analysis of MeOAzB/AMPS/MMA.

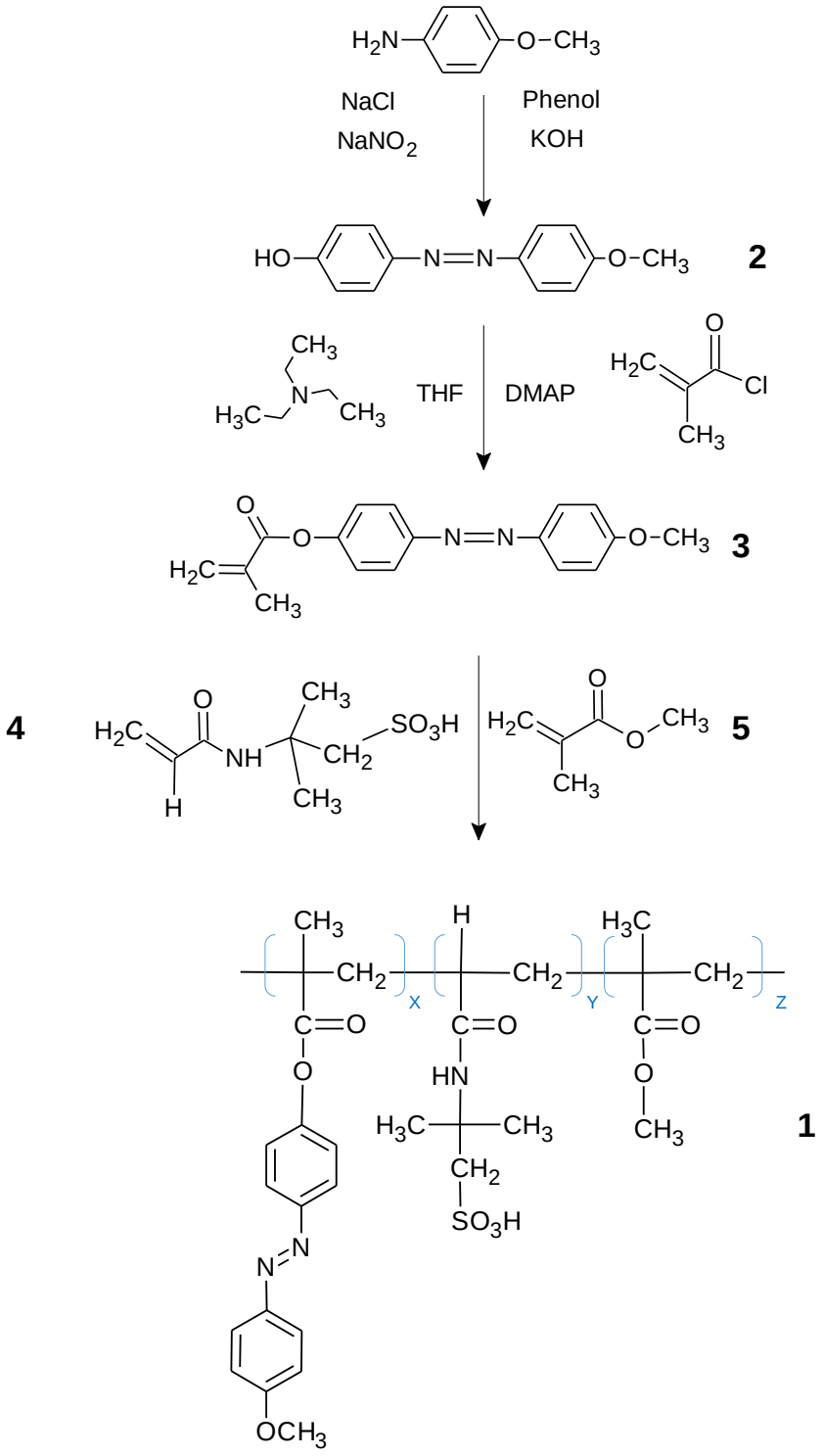

Figure 2. Synthetic route of poly[(4-methoxyazobenzene -4'-oxy) methacrylate]-*co*-poly[2-acrylamido-2-methyl-1-propanesulfonic acid]-*co*-poly[methyl methacrylate], MeOAzB/AMPS/MMA, ***1***. *X*=44, *Y*=18 and *Z*=38, represent the molar % of each monomeric unit in the polymer chain

2. Experimental section

Synthesis of poly[(4-methoxyazobenzene -4'-oxy) methacrylate]-co-poly[2-acrylamido-2-methyl-1-propanesulfonic acid]-co-poly[methyl methacrylate], MeOAzB/AMPS/MMA*, **1**.*

The MeOAzB/AMPS/MMA terpolymer was prepared following the route shown in **Fig. 2**. The synthesis of 4-hydroxy-4'-methoxyazobenzene, ***2***, is described in detail elsewhere [31-33]. N,N-dimethylaminopyridine (DMAP) (40 mg, 0.3 mmol), triethylamine (1.06 g, 10.5 mmol) and ***2*** (1.14 g, 5 mmol), were dissolved in 75 mL of THF. The mixture was cooled using ice, and methacrylic chloride (1.15 g, 11 mmol) was added dropwise. The resulting reddish solution was stirred at 40°C for 24 h, and after cooling to room temperature, the reaction mixture was poured into water and the precipitate collected and recrystallised from ethanol, obtaining 4-(methoxyazobenzene -4'-oxy) methacrylate, ***3***. Yield: 52 %; ^{1}H-NMR (DMSO-d_6, δ): 6.9 - 7.8 (m, aromatic, 8 H; *J* = 3.0, 8.9, 8.8 and 9.0 Hz), 5.7, 6.3 (s, CH_2=C-, 2H), 3.8 (s, $ArOCH_3$, 3H), 2.0 (s, $CH_3C(COO)$, 3H), see **Fig. ESI1**.

Methyl(methacrylate), MMA, ***4***, was purchased from Acros, and purified by washing with NaOH and water, followed by drying with anhydrous $MgSO_4$. 2-Acrylamido-2-methyl-1-propanesulfonic acid, AMPS, ***5*** (99% purity), was purchased from Sigma Aldrich and used without further purification. All other reagents were used as received from Sigma Aldrich.

The terpolymer MeOAzB/AMPS/MMA, ***1***, was prepared by free radical polymerisation, by dissolving ***3***, (0.6 g, 2 mmol), ***4*** (0.4 g, 2 mmol) and ***5*** (0.2 g, 2 mmol), in dimethylformamide (12.1 g), and 1,10- azobis(cyclohexane carbonitrile) (0.0132 g) was added as initiator. The reaction mixture was flushed with nitrogen for 45 min, then heated at 80^{o}C in the absence of oxygen, to initiate polymerisation. After 24 h, the reaction was terminated by precipitation into diethyl ether. The polymer was purified by subsequent precipitations from dichloromethane into diethyl ether. Yield (MeOAzB/AMPS/MMA): 65.0% in terms of MeOAzB equivalents; ^{1}H-NMR ($CDCl_3$, δ): 8.5 (s, NH, 1H) 6.9, 7.8 (m, aromatic, 8H), 3.8 (s, $ArOCH_3$, 3H), 3.6 (s, CH_3-OCO, 3H), 2.8 (s, CH_2SO_3, 2H), 2 - 0.7 (m, main chain, 7H).

Characterisation techniques

The chemical structures of the terpolymer and the intermediates were verified by nuclear magnetic resonance, ^{1}H-NMR, using a 400 MHz Bruker AVANCE III NMR spectrometer, and by infrared spectroscopy, IR, using a Perkin Elmer Spectrum One FT-IR spectrometer equipped with an Attenuated total reflectance (ATR). For the ^{1}H-NMR experiments, either deuterated chloroform ($CDCl_3$) or dimethyl sulfoxide (DMSO-d_6) was used as the solvent. IR measurements were taken on powder samples, at room temperature. The IR spectra were

obtained in the 4000 – 400 cm^{-1} range, with a 4 cm^{-1} accuracy, as the average of 64 scans. The average molecular weights, M_w and M_n, polydispersity, M_w/M_n, and degree of polymerisation, DP, of MeOAzB/AMPS/MMA, were measured using a Shimadzu 20A setup with a refractive index detector (Shimadzu RID-10A), equipped with a PL polypore column. Samples were eluted in tetrahydrofuran with a flow rate of 1 ml·min^{-1} at 25ºC. Polystyrene standards were used for calibration.

The phase behaviour of MeOAzB/AMPS/MMA was determined by differential scanning calorimetry, DSC, using a Mettler Toledo DSC1 module. Around 4 mg of the sample were heated from 25ºC to 200ºC, held at 200ºC for 3 minutes, cooled to 25ºC, held for 3 minutes, and then reheated again to 200ºC. All scans were conducted at a rate of ±10ºC·min^{-1} under nitrogen atmosphere. Phase identification was confirmed by an Olympus BX51 polarised optical microscope, POM. The thermal stability of the terpolymer was assessed by thermogravimetric analysis, TGA, using a Mettler Toledo TGA/DSC1 module from 25ºC to 800ºC, under 10 ml·min^{-1} flowrate of nitrogen.

The ultraviolet-visible (UV-Vis) absorbance spectra of MeOAzB/AMPS/MMA was recorded at room temperature, on a film cast on a quartz substrate, and in a $4.9 \cdot 10^{-5}$ M THF solution, using a Perkin Elmer Lambda 750UV-VIS-NIR spectrometer in the 200 to 800 nm wavelength range. The terpolymer samples were measured before (ground state) and immediately after (excited state) being exposed for 10 minutes with UV light (λ= 365 nm, intensity = 50 μW/cm^2). Samples were then kept in the dark, and were measured at various intervals until the spectra recovered its original shape (relaxation).

The photometric setup described in **Fig. 3** was used to study the photoanisotropy kinetics of MeOAzB/AMPS/MMA under polarised actinic light. A diode-pumped solid-state laser, DPSS, emitted linearly polarised light in the blue spectral range (445 nm wavelength), and the probing beam was generated by a laser at a 635 nm wavelength, with an angle of 45 degrees relative to the polarisation beam. The light transmitted through the terpolymer was then analysed by using an appropriate filter, with the photodetector oriented orthogonally to the polarisation direction of the probing beam, in order to record optical anisotropy. The dynamics of light response upon exposure was recorded in terms of the effective anisotropy (A_{eff}) and effective anisotropy rate ($\dot{A_{eff}} = {}^{\partial A_{eff}}/_{\partial t}$). It should be noted that the material shows minimal absorption at the probe beam wavelength (635 nm), hence, any induced linear birefringence is prominent in our experiments and dichroism effects can be neglected [34].

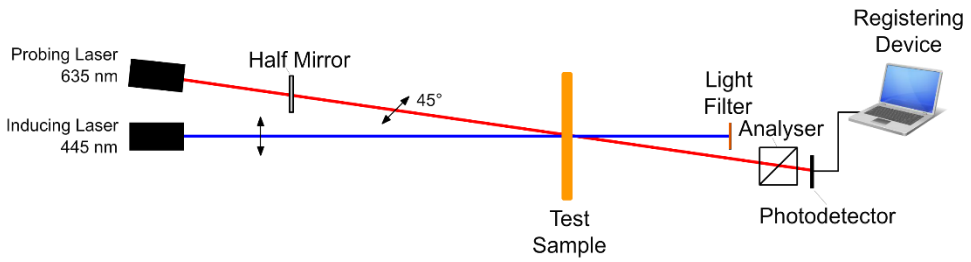

Figure 3. Experimental setup to determine the photoanisotropy kinetics of MeOAzB/AMPS/MMA.

The dielectric measurements were carried out on a metal-insulator-metal (MIM) structure device. Firstly, MeOAzB/AMPS/MMA was dissolved in dichloromethane (DCM), to yield a 5 % weight solution of the terpolymer. Glass substrates were pre-cleaned by sonicating for 10 min in soap water, acetone, isopropanol and distilled water, and dried with nitrogen gas. The clean glasses were then pre-coated with aluminium *via* thermal evaporation, and the MeOAzB/AMPS/MMA DCM solution was spin coated on the substrate to yield a homogeneous transparent thin film, which was dried in an oven at 80°C for 24 hours, in order to remove residual solvent. The thickness of the resulting film was 0.9 ± 0.1 μm, measured by a KLA Tencor P-6 mechanical profilometer. The aluminium top electrode was then deposited on the film to produce the MIM structure device, which was subsequently used for dielectric analysis. Measurements were carried out in the frequency range of 0.01 Hz to 1 MHz, by using a combination of two apparatus: a home-made dielectric spectrometer (0.01–10^4 Hz), and an Agilent 4294A impedance analyser (10^2–10^6 Hz). The spectra were obtained in isothermal steps on heating from T=-100°C to 165°C, and the isothermal frequency sweeps were performed after the sample was stabilised at the corresponding temperature for 10 min.

Cyclic voltammetry (CV) was used to calculate the molecular energy levels of MeOAzB/AMPS/MMA, using a Versa STAT 3 potentiostat in 0.1 M of potassium chloride (KCl) solution, at room temperature. 1 mM potassium ferricyanide was used as supporting electrolyte in KCl solution, ITO as the working electrode, a platinum gauze electrode as the counter electrode, and Ag/AgCl as the reference electrode. The CV measurement was carried out at 10 mV·s^{-1} scan rate.

3. Results and discussion

Structural and thermal characterisation

MeOAzB/AMPS/MMA was synthesised according to **Fig. 2**, and the molar percentages of monomeric units, *i.e.*, (4-methoxyazobenzene-4'-oxy)methacrylate, MeOAzB, *X*=44%, 2-acrylamido-2-methyl-1-propanesulfonic acid, AMPS, *Y*=18%, and methyl(methacrylate), MMA, Z=38%, were experimentally determined by ^{1}H-NMR spectroscopy and assessed by IR. More specifically, the composition was calculated using the integrals of the 7-8 ppm signal assigned to the azobenzene in MeOAzB (8H), the 2.7 ppm signal corresponding to the methylene group of AMPS (2H), and the 3.6 ppm signal associated to the methyl group of MMA (3H), see **Fig. ESI2(a)**. These results are consistent with the appearance of the corresponding IR characteristic bands in **Fig. ESI2(b)**. The molecular weight of the terpolymer was determined by GPC, **Fig. ESI2(c)**, showing unimodal distribution. Considering the lower reactivity ratio of the AMPS monomer[35, 36], we cannot rule out that MeOAzB/AMPS/MMA may contain tapered chains initiated by polymerisation of methacrylate units, and we will treat our material as a statistical terpolymer[13]. The calculated molecular weights are M_n = 66751 g·mol^{-1} and M_w = 101209 g mol^{-1}, with a polydispersity value of M_w/M_n = 1.52, and degree of polymerisation of *DP* = 326.

The thermogravimetric and derivative thermogravimetric curves of MeOAzB/AMPS/MMA (TG and DTG, respectively) are shown in **Fig. 4(a)**. Thermal decomposition of the terpolymer proceeds through two main weight loss processes: degradation of side chains, in the 250ºC/350ºC range (temperature at 5% weight loss is $T_{5\%}$~280ºC), followed by breakage of the copolymer main chain, in the 350ºC/550ºC range. This thermal degradation profile is similar to that reported on analogous 10-MeOAzB/AMPS/MMA terpolymers, ***6***, but the absence of long alkyl spacers (C_n, *n*=10) between the azobenzene group and the polymer backbone in MeOAzB/AMPS/MMA seems to destabilise its side chains[13, 37, 38].

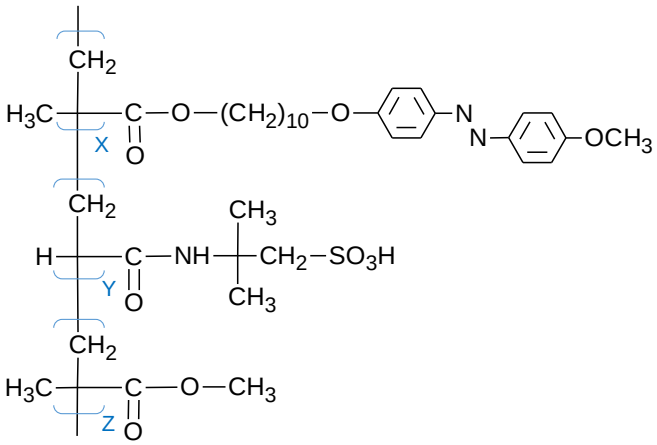

***6*,** liquid crystalline 10-MeOAzB/AMPS/MMA terpolymers reported in [13].

Fig. 4(b), on the other hand, depicts the thermogram obtained by differential scanning calorimetry, DSC, corresponding to the second heating scan of MeOAzB/AMPS/MMA. The curve displays a pseudo-second order transition, associated to the glass transition of the polymer, at T_g ~ 151ºC, and there are no visible first order thermal transitions. Polarised optical microscopy, POM, did not reveal other thermal events and we then can rule out the formation of liquid crystalline phases. The terpolymer is therefore amorphous and forms a glass at $T < T_g$.

Under some circumstances, the molecular anisotropy of the azobenene groups can promote liquid crystal behaviour, and in the past we reported the formation of smectic phases by the 10-MeOAzB/AMPS/MMA analogues, ***6*** [13, 39]. The absence of alkyl spacers in MeOAzB/AMPS/MMA, however, seems to inhibit the capability of the MeOAzB groups to decouple from the backbone motions and ultimately rearrange into mesomorphic structures[40, 41]. Due to the proximity of the azobenzene bulky groups to the main chain, the segmental motions of the polymer backbone may also be impeded, and MeOAzB/AMPS/MMA exhibits a higher glass transition compared to the 10-MeOAzB/AMPS/MMA terpolymers (T_g ~ 70ºC) [13]. This limitation in backbone mobility must be further embraced by the existence of hydrogen bonding between the AMPS groups [42], which potentially affects the MeOAzB motions too, as we will discuss with detail in the next sections.

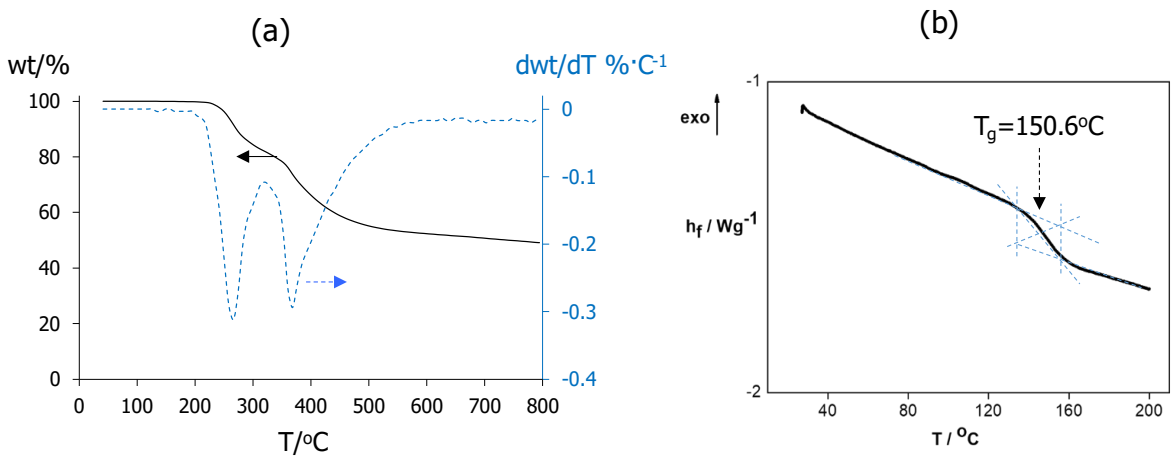

Figure 4. Thermal analysis of MeOAzB/AMPS/MMA: (a) thermogravimetric (TG, solid line) and derivative thermogravimetric (DTG, dotted line) curves; (b) differential scanning calorimetric (DSC) thermogram obtained during the second heating scan, indicating the glass transition, T_g; h_f is specific heat flow.

Light responsive behaviour

We now study the light response of the MeOAzB/AMPS/MMA terpolymer, and **Fig. 5** shows its UV-Vis spectra measured for: (a) a THF solution (tetrahydrofuran), and (b) a film cast on quartz. Prior to UV exposure, see crosses in **Fig. 5**, an intense band appears centred at ~349 nm, corresponding to the π–π^* transition of the azobenzene *trans* conformer, together with a much weaker absorption band at ~450 nm, associated with the symmetric forbidden n–π^* transition[43]. These bands confirm the light responsive behaviour of MeOAzB/AMPS/MMA, induced by the presence of the MeOAzB units, which is the majority monomeric component in the terpolymer (X=44%, molar %).

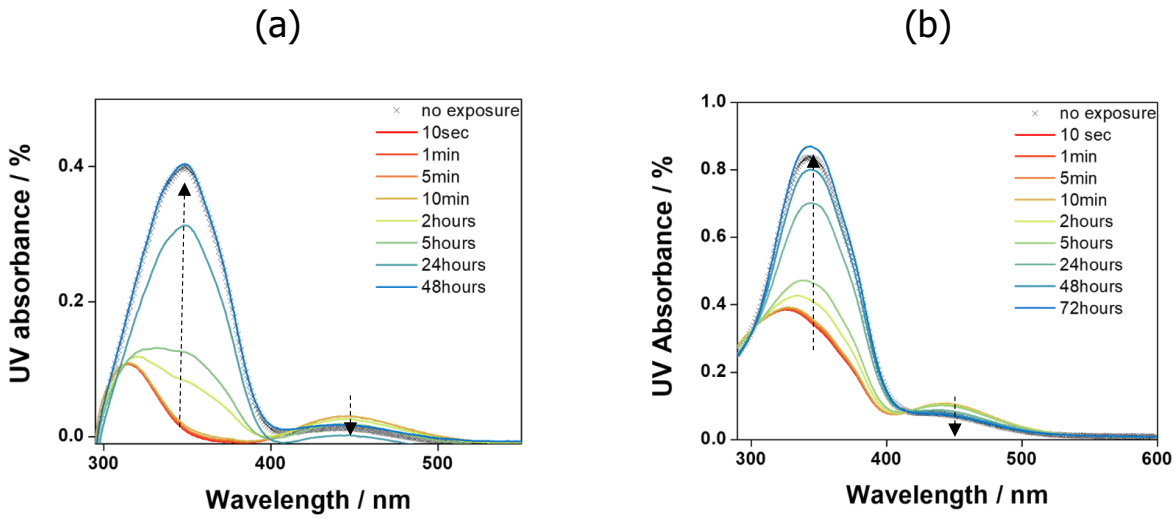

Figure 5. UV-Vis spectra of MeOAzB/AMPS/MMA obtained for: (a) a $4.9 \cdot 10^{-5}$ M THF solution; (b) a film cast on quartz. Crosses correspond to the non UV-exposed sample, and solid lines correspond to measurements taken at different relaxation times after illumination with 365 nm light for 10 minutes, keeping the sample in the dark. Dotted arrows indicate the effect of thermal relaxation.

Irradiation with light at 365 nm promotes fast *trans*-to-*cis* photoisomerisation, resulting in a dramatic increase of the π–π^* transition band, and a simultaneous (and less acute) increase of n–π^*. It is worth noting that, upon irradiation, the quartz film shows larger residual absorbance of the ~349 nm band (0.35%, **Fig. 5(b)**), compared to that observed in solution (almost zero, **Fig. 5(a)**), suggesting that a fraction of azobenzenes might not undergo *trans*-to-*cis* isomerisation in the bulk. The two samples were then kept in the dark, and the UV-Vis spectra were measured at different time intervals, in order to monitor the *cis*-to-*trans* thermal relaxation. Whilst the spectra measured in solution took 48 hours to relax back into the original state, the film needed 72 hours, evidencing that the molecular processes are slower in the bulk. We note that MeOAzB/AMPS/MMA requires longer times than the liquid crystalline 10-MeOAzB/AMPS/MMA analogues[13], probably due to the stronger coupling between the side-chain azobenzenes and the skeletal main chain.

It is clear that the photoisomerisation kinetics of MeOAzB/AMPS/MMA is highly sensitive to steric effects involving the azobenzenes[43], which may restrict the molecular mobility in the terpolymer. In principle, we could argue that such restrictions could also hinder *cis*-to-*trans* isomerisation, but the proximity of the MeOAzB units to the backbone may also induce steric strains in the *cis* form that could ultimately endow in faster thermal relaxation rates [44-46]. These two competing effects must somehow offset to yield the average light response in **Fig. 5**, and

the back relaxation process of the terpolymer follows first-order kinetics in both solution and the bulk, see **Fig. ESI3**, albeit much slower in the latter.

The effective photoanisotropy of MeOAzB/AMPS/MMA, A_{eff}, has been calculated in the form of light-induced birefringence, excluding dichroism effects [34, 47],

$$A_{eff} = \frac{1}{2}\left[1 - \cos\left(\frac{2\pi}{\lambda} d\Delta n\right)\right] \quad \text{Eq. 1}$$

where λ is the wavelength of the inducing light, *d* is the thickness of the medium, and Δn is the optical birefringence[48-50]. According to **Fig. 6(a)**, MeOAzB/AMPS/MMA shows a limited degree of light induced birefringence. Its response has been compared to those of a solid solution with the azo-chromophore non-covalently bound to the polymer matrix, MY-26, ***7***, and a polymer with nitro-azomonomers built-in, BiN-GP, ***8***, [28]

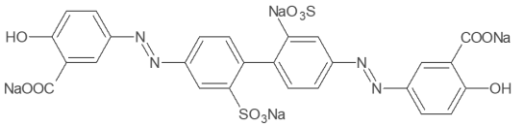

7, MY-26

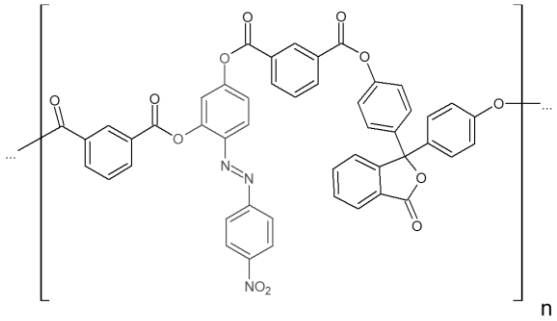

8, BiN-GP

The A_{eff} values of MeOAzB/AMPS/MMA fall between those exhibited by MY-26 and BiN-GP. Interestingly, and compared to these model compounds, our terpolymer shows very high photoanisotropy induction rate, $\dot{A_{eff}}$, calculated as the derivative of A_{eff} at the initial moments of isomerisation, see **Fig. 6(b)**,

$$\dot{A_{eff}} = {}^{\partial A_{eff}}/_{\partial t} \quad \text{Eq. 2}$$

These results demonstrate the sensitivity of MeOAzB/AMPS/MMA to actinic radiation, and therefore its potential to be used in linearly polarised systems, but also confirm the limited isomerisation efficiency of the azobenzenes in this terpolymer. It is worth mentioning that the

UV-Vis absorbances of MY-26 and BiN-GP at ν = 445 nm are similar to that of MeOAzB/AMPS/MMA, see **Fig. 5(b)** and **Fig. ESI4**, suggesting that the corresponding photoanisotropies are comparable.

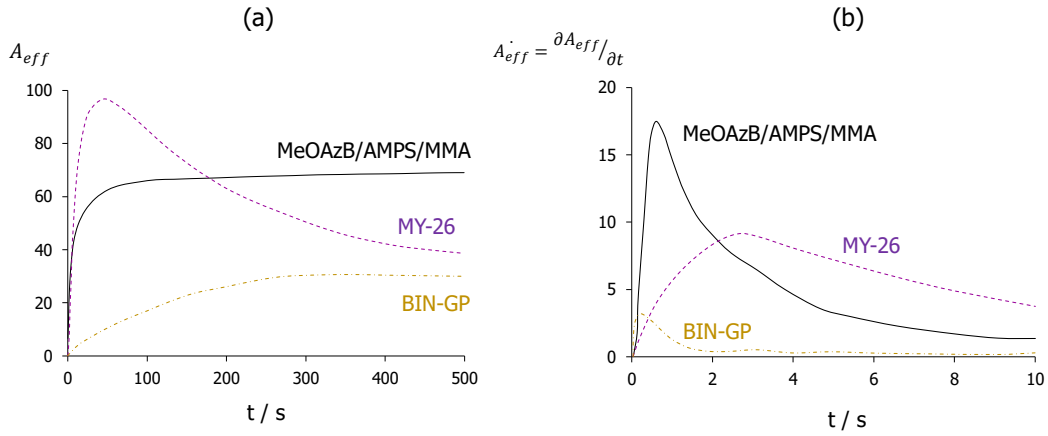

Figure 6. Kinetic curves corresponding to the photoanisotropy induction of MeOAzB/AMPS/MMA (solid line) and two reference materials (MY-26 and BIN-GP, dotted lines): (a) effective anisotropy, A_{eff}; (b) effective anisotropy rate immediately after light application (t = 10 s), $\dot{A_{eff}}$.

We believe that the photonic response of MeOAzB/AMPS/MMA must be substantially enhanced by the strong electrostatic interactions between the sulfonic acids and the azobenzenes [51]. More specifically, **Fig. 6** suggests that the sulfonic groups in MeOAzB/AMPS/MMA promote more effective light response than the dense network of ester linkages (CO.O) and the nitro terminations (NO_2) in BIN-GP. The high A_{eff} values can be then explained by the ionisable character of the SO_3H groups, compared to the partial polarisation achieved by CO.O and NO_2 [52]. Whilst MeOAzB/AMPS/MMA shows smaller A_{eff} values than MY-26, the terpolymer presents greater design flexibility, since the relative position of the sulfonic and the azobenzene units can be tailored, at least to some extent. Ultimately, the preparation of azo-polymers offers the exciting possibility to tune the light response *via* polymerisation parameters, such as, monomer composition and distribution, molecular weight or polymerisation degree [53, 54]. The high photoanisotropy induction rate exhibited by MeOAzB/AMPS/MMA, $\dot{A_{eff}}$, will be further discussed during the next sub-section.

Molecular mobility and conductivity. Dielectric response

We now apply dielectric spectroscopy with the aim to correlate the light-response of MeOAzB/AMPS/MMA to the local environment of the azobenzene groups in the terpolymer

structure. The temperature-frequency dependence of the dielectric loss factor, ε'', is summarised in **Fig. 7(a)**, displaying several dielectric processes illustrated in **Fig. 8**. More specifically, five relaxations, associated to dipole reorganisations, are observed and are labelled as γ, β, βx, α and δ, in increasing temperature order, see **Fig. 7(a)** and **7(b)**. At low temperatures, -100ºC/50ºC , the γ and β relaxations are visible and are assigned to motions of the terminal methoxy and azobenzene groups, respectively, in the MeOAzB chains [55, 56]. In the high temperatures range, T ≥150ºC, the α relaxation is observed, corresponding to the onset of main-chain segmental motions, and associated to the glass transition of the terpolymer (T_g). At higher temperatures, T>T_g, more free volume is available, and the δ relaxation is activated, associated to the rotation of the MeOAzB side chains along the main chain axis [56]. This process has been ascribed previously to the onset of direct current, DC, conductivity through smectic phases in azobenzene-based polymers[15], and we will return to this observation later.

These relaxations (γ, β, α and δ) are typical of comb-shaped poly(methacrylate)s [55, 57-60], and we note that the so-called β1 relaxation was not unveiled in our measurements, normally ascribed to flip-flop motions of the polarisable carboxyl groups (CO.O) that activate the α relaxation in the glass state[61-63]. Instead, we have observed an additional relaxation at intermediate temperatures between the β and α processes, see **Fig. 7(b)** for tan(δ)=ε''/ε'. This process, hereinafter labelled as βx, is not observed in other polymers containing only MeOAzB and/or MMA units[15], and must be then associated to the presence of AMPS groups. Unfortunately, it was not possible to monitor βx through the whole experimental temperature-frequency range, probably due to the low concentration of sulfonic groups in the terpolymer (*Y*=18%).

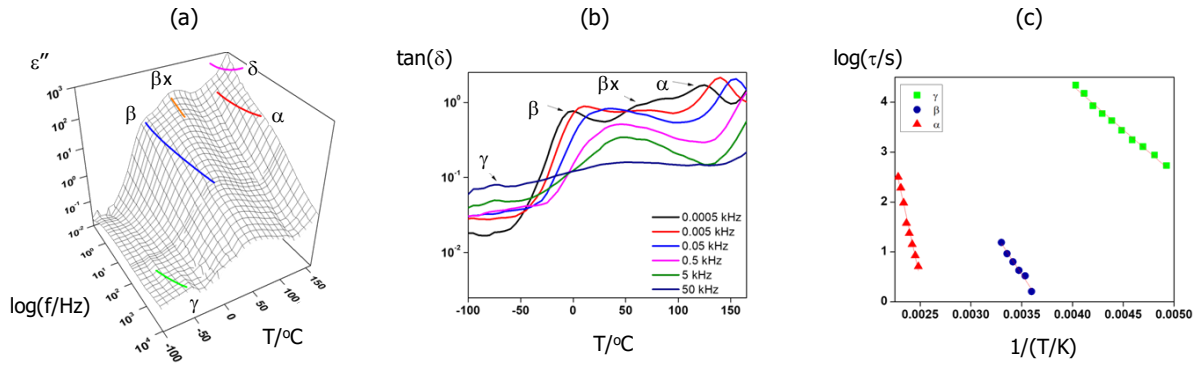

Figure 7. Summary of the dielectric response of MeOAzB/AMPS/MMA: (a) temperature and frequency dependence of the loss factor, ε''; (b) temperature dependence of tan(δ)=ε''/ε' at

selected frequencies; (c) Arrhenius plots showing the relaxation times, τ, corresponding to the maxima in the ε'' curves for different relaxations.

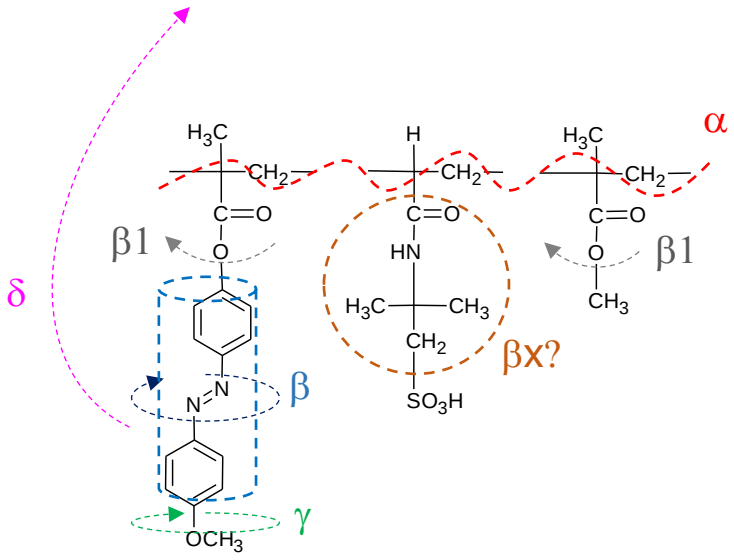

Figure 8. Schematic representation of the dielectric relaxations (γ, β, βx, β1, α and δ) and molecular motions of MeOAzB/AMPS/MMA (β1was not observed experimentally in this work[15]).

We have studied the thermal activation of the γ, β and α dielectric processes *via* their relaxation times, corresponding to the maxima of the ε'' curves obtained after fitting the experimental results to a sum of empirical Havriliak-Negami (HN) functions[64],

$$\varepsilon^*(i\omega) = \varepsilon_\infty + \sum_k \frac{\Delta\varepsilon}{(1+(i\omega\tau)^m)^n} + \frac{\sigma_{dc}}{(i\omega)^p} \qquad \text{Eq. 3}$$

where ω is the angular frequency, ε_∞ is the instantaneous permittivity, $\Delta\varepsilon$ is the dielectric relaxation strength, τ is the relaxation time, *m* and *n* are parameters describing the width and asymmetry of the distribution of relaxation times, *k* is the number of relaxations, σ_{dc} is the direct current conductivity and *p* is a parameter describing the contribution of conductivity to the dielectric permittivity. $i = \sqrt{-1}$ is the imaginary unit. Both γ and β processes show Arrhenius behaviour, see **Fig. 7(c)**, and their activation energies, E_a, can be obtained according to,

$$\tau(T)_{max} = \tau_o \exp(\frac{E_a}{R} \cdot \frac{1}{T}) \quad \text{Eq. 4}$$

where $\tau_o = \tau_{max}$ at $T \to \infty$, and R is the absolute gas constant. The results for MeOAzB/AMPS/MMA are summarised in **Table 1**, and both relaxations show slightly higher E_a values than other analogous azo-polymers that contain flexible spacers, the 10-MeOAzB/AMPS/MMA terpolymers discussed above. This may reflect the motional restrictions of the MeOAzB units in our terpolymer compared to comb-shaped poly(methacrylate)s [15]. The linearity of the γ and β processes in **Fig. 7(c)** is consistent with their predominant local character, even though the high E_a values denote some sort of cooperativity by the influence of the intermolecular environment on the dielectric response. Our results are also consistent with the activation energy values obtained for epoxy-based oligomers containing nitroazobenzene chromophore fragments, labelled as FIII, CFAO and CFMAO in **Table 1**, and whose structures are shown in **Fig. ESI5** [65, 66].

Contrarily, the τ-temperature dependence of the α process clearly deviates from linearity, and can be described by the Vogel-Fulcher-Tamman equation[67, 68],

$$\tau(T)_{max} = \tau_o \exp(\frac{B}{T - T_0}) \quad \text{Eq. 5}$$

where τ_0 represents the pre-exponential term, T_0 is the Vogel temperature, which is associated to the cessation of motions of polymeric segments, and B is an apparent activation energy. The high B value confirms the complex phenomena associated to this relaxation, which involve segmental motions in the MeOAzB/AMPS/MMA main chain. These motions may be impeded by the presence of the bulky MeOAzB units and the formation of hydrogen bonds by the AMPS groups, as mentioned above.

Table 1. Kinetic parameters of the different dielectric relaxation processes in MeOAzB/AMPS/MMA, according to Eq. 4 and 5. We include values obtained for reference comb-shaped poly(methacrylate)s (see structures in **Fig. ESI5**).

	γ- process		β- process		α- process		
Sample acronym*	**-log(τ_o/s)**	**E_a (kJ·mol^{-1})**	**-log (τ_o/s)**	**E_a (kJ·mol^{-1})**	**-log(τ_o/s)**	**B (K)**	**T_o (K)**
MeOAzB/AMPS/MMA	11.2	32.9	11.4	59.1	17.9	1705	300
0.22MeOAzB/MMA[15]	16.7	34.7	16.7	54.6	17.3	868	305
FIII[65]	-	-	14.2	46.0	11.7	2698	274
CFAO[66]	12.4	26.8	16.5	61.9	10.9	1496	336
CFMAO[66]	12.3	25.1	15.9	51.9	9.7	1279	318

* As per the corresponding references.

The δ relaxation, on the other hand, could not be analysed with detail in our experimental temperature range, but can be associated to the onset of DC conductivity processes [15], σ_{dc}, which we have studied through the real component of the complex conductivity, $\sigma^* = \sigma' + i\sigma''$,

$$\sigma' = \omega \varepsilon_O \varepsilon'' \qquad \text{Eq. 6}$$

where $\varepsilon_O = 8.85 \cdot 10^{-12}\ F\ \cdot m^{-1}$ is the permittivity of free space.

The log(σ') *vs* log(f/Hz) plots of MeOAzB/AMPS/MMA are depicted in **Fig. 9**, between T=-10ºC and T=165ºC. The low conductivity values could be somehow expected, considering the small concentration of polarisable sulfonic groups in the terpolymer (*Y*=18%). At high temperatures, a DC process, $\sigma_{dc,1}$, is distinguishable at around T~140ºC from the plateaus in **Fig. 9**. This process is ascribed to the α relaxation related to the onset of segmental motions in the polymer backbone occurring near the glass transition.

Interestingly, at lower temperatures, T=35ºC, the log(σ') curves start to develop inflexions in the low frequency range, suggesting the presence of an additional direct current conductivity process, $\sigma_{dc,2}$. The temperature-frequency range of this DC process is similar to the so-called βx relaxation, and we believe that the $\sigma_{dc,2}$ conductivity could be then ascribed to dipole reorganisations of AMPS groups that are locally activated in the polymer glass, at T < T_g, hence ascribed to the sulfonic acids in the terpolymer. It is possible that such local conductivity effects facilitate motions of the azobenzenes in the terpolymer (responsible of the β relaxation) and ultimately enhance the photoanisotropy induction rate, $\dot{A_{eff}}$. Both

conductivity processes, $\sigma_{dc,1}$ and $\sigma_{dc,2}$, are further promoted in the vicinity of the glass transition, T_g=150ºC, by the increase of free volume available around the main chain.

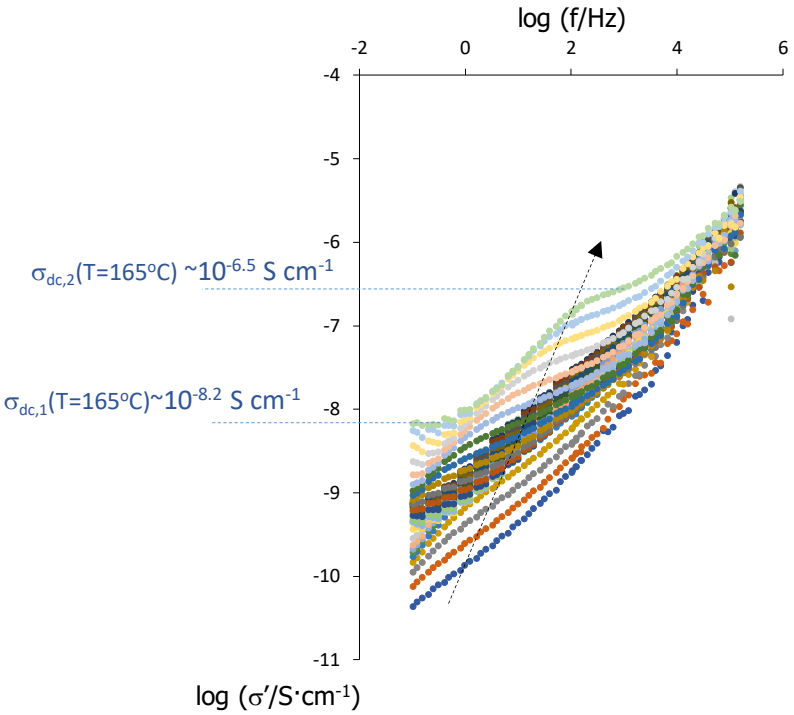

Figure 9. Double logarithmic plots of the real component of the complex conductivity, σ′, of MeOAzB/AMPS/MMA, as a function of the frequency, measured in isothermal steps (°C) on heating from the glass (T=-10ºC) to the rubbery state (T=165ºC); estimation of $\sigma_{dc,1}$ and $\sigma_{dc,2}$ at T=165°C. Dotted arrow indicates direction on heating.

The relationships between MeOAzB/AMPS/MMA molecular mobility and conductivity are now further investigated by its electrochemical response and molecular energy levels, *via* cyclic voltammetry, CV, see **Fig. 10(a)**. The highest occupied molecular orbital (HOMO), lowest unoccupied energy levels (LUMO) and the electrochemical band gap (E_g^{el}) were determined by taking the known E_{HOMO} of ferrocene (Fc) (4.8 eV below the vacuum level) as reference value,

$$E_{HOMO} = -e[E_{OX/RED} + 4.8 - E_{FOC}] \quad \text{Eq. 7}$$

$$E_{LUMO} = E_{HOMO} + E_g^{el} \quad \text{Eq. 8}$$

where $E_{OX/RED}$ is the first onset oxidation and reduction potential of MeOAzB/AMPS/MMA and E_{FOC} is the external standard potential of ferrocene/ferrocenium (Fc/Fc^+) ion couple. The E_{FOC} was measured to be 0.16 eV in KCl solution. E_{HOMO} = -5.37 eV and E_{LUMO} = -3.42 eV, are the HOMO and the LUMO energy levels, respectively, where the onset oxidation is E_{OX} = 0.57 V and the onset reduction is E_{RED} = -1.38 V, obtained from the potential curves of the polymer. Reduction starts from the electron transporting segments, which are most probably the N atoms in the azobenzene chromophore and AMPS, while we believe that oxidation must start from the hole transporting segments located at the sulfonic terminations. The electrochemical band gap calculated from the HOMO/LUMO is E_g^{el}~1.95 eV, and the energy band diagram of MeOAzB/AMPS/MMA is proposed in **Fig. 10(b)**.

An optical band gap of $E_g^{opt} = 3.03\ \text{eV}$ can also be calculated from the onset of the UV-Vis absorption spectra,

$$E_g^{opt} = \mathrm{h}\frac{\mathrm{c}}{\lambda_{\mathrm{Edge}}} \qquad \text{Eq. 9}$$

where *h* is the Planck constant, *c* is the speed of light and λ_{Edge} = 409 nm is the terpolymer optical absorbance band edge obtained from the spectra. The larger value of E_g^{opt} (respect to E_g^{el}) can probably be explained by reduction and oxidation progressing in the full conjugated system, rather than in isolated electron and hole transporting [69, 70], and hence, the bandgap measured directly from the CV might be underestimated.

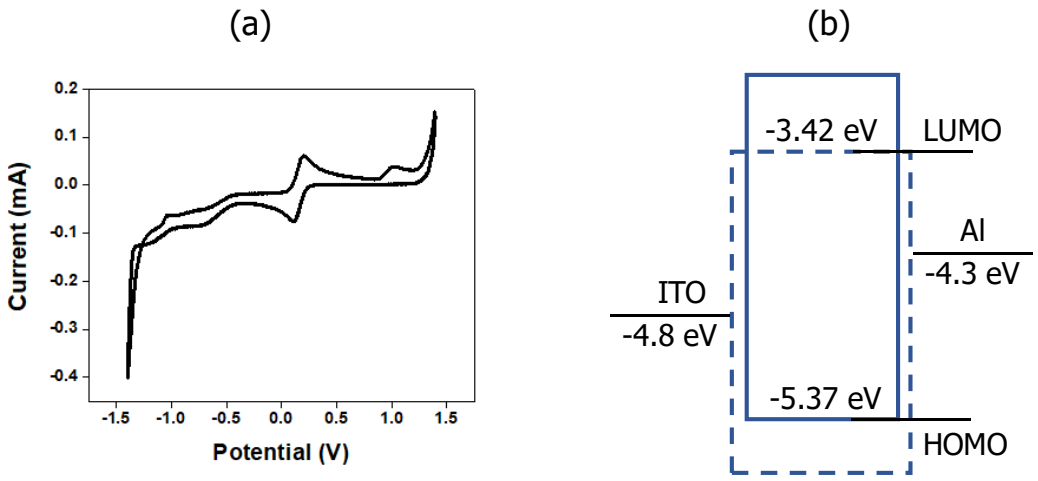

Fig. 10. (a) Cyclic voltammogram of a MeOAzB/AMPS/MMA film coated on ITO substrate, on 1 mM $K_4Fe(CN)_6$ in 0.1 M potassium chloride solution; sweep rate 10 $mV \cdot s^{-1}$; (b) Energy band diagram (hole transporting segments, –; electron transporting segments, ---).

4. Conclusions

The MeOAzB/AMPS/MMA terpolymer exhibits promising light-responsive behaviour in the glass phase ($T<T_g$), driven by *trans*-to-*cis* photoisomerisation of the methoxyazobenzene units, triggered by actinic UV light exposure at 356 nm. Our results suggest that the high photoanisotropic rate observed for MeOAzB/AMPS/MMA, $\dot{A_{eff}}$, may be promoted by interactions between the MeOAzB and AMPS units, located in different side-chains of the terpolymer structure, and associated to p-type conductivity involving the polarisable sulfonic groups of AMPS.

Even though it is challenging to draw conclusions on the molecular dynamic processes in non-equilibrium glasses[43, 71], our results open new fronts to optimise the photoresponse of azo-polymers for optoelectronic applications. More specifically, the role of the polymer backbone rigidity and chemical composition, the inclusion of liquid crystalline phases *via* block-copolymerisation, the promotion of hydrogen bonding[72], and the molecular origin and optimisation of the newly reported sub-glass βx process, will be the focus of new investigations taking MeOAzB/AMPS/MMA as a reference.

Acknowledgements

This work was supported by the University Malaya under the UMRG grant RP038B-17AFR. NFKA and AMF would like to thank the Royal Academy of Engineering, U.K., and Academy of Science, Malaysia, for the grant NRCP1516/4/61, from the Newton Research Collaboration Programme, and the University of Aberdeen, for the award of the grant SF10192, corresponding to the Global Challenge Research Fund Internal Pump Priming Fund Round 2. AMF would like to acknowledge the Carnegie Trust for the Universities of Scotland for the award of one Scottish Research Incentive Grant (RIG008586).

References

1 Natansohn A, Rochon P. Photoinduced motions in azo-containing polymers. Chem. Rev. 2002; 102; 4139-75.

2 Bandara HMD, Burdette SC. Photoisomerization in different classes of azobenzene. Chem. Soc. Rev. 2012;41; 1809-25.

3 Ichimura K. Photoalignment of liquid-crystal systems. Chem. Rev. 2000 MAY;100(5):1847-73.

4 Hagen R, Bieringer T. Photoaddressable polymers for optical data storage. Adv. Mater. 2001, 13; 1805-10.

5 Forcen P, Sanchez C, Rodriguez FJ, Alcala R, Oriol LT, Hvilsted S, Jankova K, Loos J. Pulsed holographic gratings in azo-polymethacrylates with different molecular architectures. Practical Holography XXI: Materials and Applications 2007;6488; 48807-.

6 Matharu AS, Jeeva S, Ramanujam PS. Liquid crystals for holographic optical data storage. Chem. Soc. Rev. 2007;36; 1868-80.

7 Gindre D, Boeglin A, Fort A, Mager L, Dorkenoo KD. Rewritable optical data storage in azobenzene copolymers. Opt. Express 2006; 16;9896-901.

8 Royes J, Provenzano C, Pagliusi P, Tejedor RM, Pinol M, Oriol L. A bifunctional amorphous polymer exhibiting equal linear and circular photoinduced birefringences. Macromol. Rapid. Commun. 2014; 35; 1890-5."

9 Lomba M, Oriol L, Sanchez C. A new photoimaging system based on a trisdiazonium salt as a photocrosslinker for sulfonated polyelectrolytes. Eur. Polym. J. 2009; 45; 1785-90.

10 Berges C, Oriol L, Pinol M, Sanchez-Somolinos C, Alcala R. Blends of an azomethacrylic block copolymer for volume holographic storage using low energy 10 ms light pulses. Opt. Mater. 2013; 35; 1095-8.

11 Forcen P, Oriol L, Sanchez C, Rodriguez FJ, Alcala R, Hvilsted S, Jankova K. Volume holographic storage and multiplexing in blends of PMMA and a block methacrylic azopolymer, using 488 nm light pulses in the range of 100 ms to 1 s. Eur. Polym. J. 2008; 44; 72-8.

12 Yu H, Jiang M, Guo Y, Turiv T, Lu W, Ray V, Lavrentovich OD, Wei Q. Plasmonic metasurfaces with high UV-vis transmittance for photopatterning of designer molecular orientations. Adv. Opt. Mater. 2019; 7; 1900117.

13 Vanti L, Mohd Alauddin S, Zaton D, Aripin NFK, Giacinti-Baschetti M, Imrie CT, Ribes-Greus A, Martinez-Felipe A. Ionically conducting and photoresponsive liquid

crystalline terpolymers: Towards multifunctional polymer electrolytes. Eur. Polym. J. 2018; 109; 124-32.

14 Martinez-Felipe A, Lu Z, Henderson PA, Picken SJ, Norder B, Imrie CT, Ribes-Greus A. Synthesis and characterisation of side chain liquid crystal copolymers containing sulfonic acid groups. Polymer 2012; 53; 2604-12.

15 Martinez-Felipe A, Santonja-Blasco L, Badia JD, Imrie CT, Ribes-Greus A. Characterization of functionalized side-chain liquid crystal methacrylates containing nonmesogenic units by dielectric spectroscopy. Ind. Eng. Chem. Res. 2013; 52; 8722-31.

16 Martinez-Felipe A, Badia JD, Santonja-Blasco L, Imrie CT, Ribes-Greus A. A kinetic study of the formation of smectic phases in novel liquid crystal ionogens. Eur. Polym. J. 2013; 49; 1553-63.

17 Martinez-Felipe A, Imrie CT, Ribes-Greus A. Study of structure formation in side-chain liquid crystal copolymers by variable temperature fourier transform infrared spectroscopy. Ind. Eng. Chem. Res. 2013; 52; 8714-21.

18 Martinez-Felipe A. Liquid crystal polymers and ionomers for membrane applications. Liq. Cryst. 2011; 38; 1607-26.

19 Concellon A, Claveria-Gimeno R, Velazquez-Campoy A, Abian O, Pinol M, Oriol L. Polymeric micelles from block copolymers containing 2,6-diacylaminopyridine units for encapsulation of hydrophobic drugs. RSC Adv. 2016;6; 24066-75.

20 Concellon A, Blasco E, Martinez-Felipe A, Carlos Martinez J, Sics I, Ezquerra TA, Nogales A, Pinol M, Oriol L. Light-responsive self-assembled materials by supramolecular post-functionalization via hydrogen bonding of amphiphilic block copolymers. Macromolecules 2016; 25; 7825-36.

21 Jose Clemente M, Maria Tejedor R, Romero P, Fitremann J, Oriol L. Photoresponsive supramolecular gels based on amphiphiles with azobenzene and maltose or polyethyleneglycol polar head. New. J. Chem. 2015; 39; 4009-19.

22 Blasco E, Luis Serrano J, Pinol M, Oriol L. Light responsive vesicles based on linear-dendritic block copolymers using azobenzene-aliphatic codendrons. Macromolecules 2013;46; 5951-60.

23 Blasco E, Schmidt BVKJ, Barner-Kowollik C, Pinol M, Oriol L. Dual thermo- and photo-responsive micelles based on miktoarm star polymers. Polym. Chem. 2013;4; 4506-14.

24 Dong L, Feng Y, Wang L, Feng W. Azobenzene-based solar thermal fuels: Design, properties, and applications. Chem. Soc. Rev. 2018; 47.

25 Feng W, Li S, Li M, Qin C, Feng Y. An energy-dense and thermal-stable bis-azobenzene/hybrid templated assembly for solar thermal fuel. J. Mater. Chem. A 2016; 4; 8020-8.

26 Chaganava I, Chedia R, Wei Q. Study of the photoanisotropic properties of polarization sensitive compositions based on organic chromophore salts with various alkali metals. Opt. Manufact. Test XII 2018;10742:UNSP 107421K.

27 Kilosanidze B, Kakauridze G. Polarization-holographic gratings for analysis of light. 1. analysis of completely polarized light. Appl. Opt. 2007; 46; 1040-9.

28 Chaganava I, Kilosanidze B, Kakauridze G, Oriol L, Pinol M, Martinez-Felipe A. Induction of the vector polyphotochromism in side-chain azopolymers. J. Photochem. Photobiol. A 2018; 354; 70-7.

29 Soberats B, Uchida E, Yoshio M, Kagimoto J, Ohno H, Kato T. Macroscopic photocontrol of ion-transporting pathways of a nanostructured imidazolium-based photoresponsive liquid crystal. J. Am. Chem. Soc. 2014; 136; 9552-5.

30 Kato T, Yoshio M, Ichikawa T, Soberats B, Ohno H, Funahashi M. Transport of ions and electrons in nanostructured liquid crystals. Nat. Rev. Mater. 2017 2; 17001.

31 Imrie C, Karasz FE, Attard GS. The effect of molecular-weight on the thermal-properties of polystyrene-based side-chain liquid-crystalline polymers. J. Macromol. Sci. Part A: Pure Appl. Chem. 1994; A31; 1221-32.

32 Craig A, Imrie C. Effect of spacer length on the thermal-properties of side-chain liquid-crystal poly(methacrylate)s. J. Mater. Chem. 1994; 4; 1705-14.

33 Schleeh T, Imrie CT, Rice D, Karasz FE, Attard GS. Ultrastructure studies of polystyrene-based side-chain liquid-crystalline copolymers containing charge-transfer groups. J. Polym. Sci. Part A: Polym. Chem. 1993; 31; 1859-69.

34 Chaganava I, Kobulashvili I, Alauddin SM, Aripin NFK, Martinez-Felipe A Light-inducing birefringence of organic photoanisotropic materials integrated via covalent bonds. ORGANIC PHOTONIC MATERIALS AND DEVICES XXI Proc. of SPIE; 2019; 1091517.

35 Mishra A, Choudhary V. Synthesis, characterizations and thermal behavior of methyl methacrylate and N-(p-carboxyphenyl) methacrylamide/arylamide copolymers. J. Appl. Polym. Sci. 2000; 78; 259-67.

36 Talpur M, Oracz P, Kaim A. Study of methyl methacrylate-acrylamide copolymerization system in cyclohexanone in the absence of conventional radical initiator. Polymer 1996; 37; 4149-54.

37 Ferriol M, Gentilhomme A, Cochez M, Oget N, Mieloszynski J. Thermal degradation of poly(methyl methacrylate) (PMMA): Modelling of DTG and TG curves. Polym. Degrad. Stab. 2003; 79; 271-81.

38 Wang Y, Ma X, Zhang Q, Tian N. Synthesis and properties of gel polymer electrolyte membranes based on novel comb-like methyl methacrylate copolymers. J. Membr. Sci. 2010; 349; 279-86.

39 Martinez-Felipe A, Lu Z, Henderson PA, Picken SJ, Norder B, Imrie CT, Ribes-Greus A. Synthesis and characterisation of side chain liquid crystal copolymers containing sulfonic acid groups. Polymer 2012; 53; 2604-12.

40 Shibaev VP. Liquid-crystalline polymers: Past, present, and future. Polym. Sci. Ser. A 2009; 51; 1131-93.

41 Cook AG, Inkster RT, Martinez-Felipe A, Ribes-Greus A, Hamley IW, Imrie CT. Synthesis and phase behaviour of a homologous series of polymethacrylate-based side-chain liquid crystal polymers. Eur. Polym. J. 2012; 48; 821-9.

42 Pebalk D, Barmatov E, Shibayev V. Liquid crystalline ionomers as a new class of mesomorphous polymeric systems. USP. Khim. 2005;74; 610-33.

43 Kumar G, Neckers D. Photochemistry of azobenzene-containing polymers. Chem. Rev. 1989; 89; 1915-25.

44 Kamogawa H. Redox behavior in photochromic polymers of thiazine series. J. Appl. Polym. Sci. 1969; 13; 1883.

45 Kamogawa H, Kato M, Sugiyama H. Syntheses and properties of photochromic polymers of azobenzene and thiazine series. J. Polym. Sci. Part A-1: Polym. Chem. 1968;6; 2967.

46 Kamogawa H. Syntheses and properties of photochromic polymers of mercury thiocarbazonate series. J. Polym. Sci. Part A-1: Polym. Chem. 1971;9; 335.

47 Chaganava I, Kakauridze G, Kilosanidze B, Mshvenieradze Y. Vector photochromism in polarization-sensitive materials. Opt. Lett. 2014; 39; 3841-4.

48 Balabanov A, Karauridze G, Kakichashvili S, Savitsky A, Shaverdova V, Shvaitser Y. On the study of photoanisotropy spectral characteristics. Opt. Spektrosk. 1989; 67; 409-12.

49 Zhong Q, Zou L, Wang Y, Sui N, Liu Q, Zhang L, Zhang H. Photo-induced birefringence of azo-dye based on three-dimensional opal photonic crystals. Chem. Res. Chin. Univ. 2016; 32; 1063-8.

50 Jones R. A new calculus for the treatment of optical systems I. description and discussion of the calculus. J. Opt. Soc. Am. 1941; 31; 488-93.

51 Chaganava I, Kilosanidze B, Kakauridze G, Kobulashvili I. The study of polyelectrolyte-containing photoanisotropic compositions. Light Manipulating Organic Materials and Devices IV 2017;10360:UNSP 103600L.

52 Chaganava I, Kakauridze G, Kilosanidze B. Photoanisotropy in polarization-sensitive medium developed on the basis of polar water-soluble components. Practical Holography XZV: Materials and Applications 2011;795714.

53 Royes J, Rebole J, Custardoy L, Gimeno N, Oriol L, Tejedor RM, Pinol M. Preparation of side-chain liquid crystalline azopolymers by CuAAC postfunctionalization using bifunctional azides: Induction of chirality using circularly polarized light. J. Polym. Sci. Part A: Polym. Chem. 2012;50; 1579-90.

54 Blasco E, Pinol M, Berges C, Sanchez-Somolinos C, Oriol L. Smart polymers for optical data storage. Book Series: Woodhead Publishing in Materials. 2014; 510-548

55 Zentel R, Strobl G, Ringsdorf H. Dielectric-relaxation of liquid-crystalline polyacrylates and polymethacrylates. Macromolecules 1985;18; 960-5.

56 Colomer F, Duenas J, Ribelles J, Barralesrienda J, Deojeda J. Side-chain liquid-crystalline poly(n-maleimides) .5. dielectric-relaxation behavior of liquid-crystalline side-chain and amorphous poly(n-maleimides) - a comparative structural study. Macromolecules 1993; 26; 155-66.

57 Nikonorova N, Borisova T, Barmatov E, Pissis P, Diaz-Calleja R. Dielectric relaxation and thermally stimulated discharge currents in liquid-crystalline side-chain polymethacrylates with phenylbenzoate mesogens having tail groups of different length. Macromolecules 2003; 36; 5784-91.

58 Nikonorova NA, Smirnov NN, Kudryavtsev VV, Yakimanskii AV. Local forms of molecular mobility in comb-shaped chromophore-containing copoly(methacrylates). Polym. Sci. Ser. A 2008; 50; 911-9.

59 Nikonorova N, Borisova T, Barmatov E, Pissis P, Diaz-Calleja R. Comparative dielectric and TSDC studies of molecular mobility in liquid-crystalline side-chain poly(methacrylate). Polymer 2002;43; 2229-38.

60 Mano J. Cooperative character of the relaxation processes in a side-chain liquid crystalline polymer. J. Macromol. Sci. Part B: Phys. 2003;B42; 1169-82.

61 Ribes Greus A, Soria V, Figueruelo J, Diaz Calleja R. Dielectric and dynamic mechanical relaxations in methyl-methacrylate and methyl isopropenyl ketone copolymers. Polymer 1988; 29; 981-6.

62 Ribes Greus A, Soria V, Figueruelo J, Diaz Calleja R. Study of the molecular-origin of the mechanical and dielectric-beta relaxation of methyl-methacrylate isopropenyl methyl ketone copolymers. Makromol. Chem. Macromol. Symp. 1988; 20-1; 409-16.

63 Ribes Greus A, Gomez Ribelles J, Diaz Calleja R. Dielectric and mechanical dynamical studies on poly(cyclohexyl methacrylate). Polymer 1985;26; 1849-54.

64 Havrilia.S, Negami S. A complex plane representation of dielectric and mechanical relaxation processes in some polymers. Polymer 1967;8; 161.

65 Nikonorova NA, Balakina MY, Fominykh OD, Sharipova AV, Vakhonina TA, Nazmieva GN, Castro RA, Yakimansky AV. Dielectric spectroscopy and molecular modeling of branched methacrylic (co)polymers containing nonlinear optical chromophores. Mater. Chem. Phys. 2016; 181; 217-26.

66 Nikonorova NA, Balakina MY, Fominykh OD, Pudovkin MS, Vakhonina TA, Diaz-Calleja R, Yakimansky AV. Dielectric spectroscopy and molecular dynamics of epoxy oligomers with covalently bonded nonlinear optical chromophores. Chem. Phys. Lett. 2012; 552; 114-21.

67 Vogel H. The temperature dependence law of the viscosity of fluids. Phys. Z. 1921;22; 645-6.

68 Fulcher G. Analysis of recent measurements of the viscosity of glasses - reprint. J. Am. Ceram. Soc. 1992; 75; 1043-59.

69 Hwang S, Chen Y. Synthesis and electrochemical and optical properties of novel poly(aryl ether)s with isolated carbazole and p-quaterphenyl chromophores. Macromolecules 2001; 34; 2981-6.

70 Chen S, Hwang S, Chen Y. Photoluminescent and electrochemical properties of novel copoly(aryl ether)s with isolated fluorophores. J. Polym. Sci. Part A: Polym. Chem. 2004; 42; 883-93.

71 Imrie C, Ingram M, McHattie G. Ion transport in glassy polymer electrolytes. J. Phys. Chem. B 1999 MAY; 103; 4132-8.

72 Martinez-Felipe A, Brown AW. Ionic conductivity mediated by hydrogen bonding in liquid crystalline 4-n-alkoxybenzoic acids. J. Mol. Struct. 2019;1197; 487-96.